Abdominal Radiology

Published online: 1 August 2018

Abdom Radiol (2019) 44:272–278
https://doi.org/10.1007/s00261-018-1715-9

Temporal changes in MRI appearance of the prostate after focal ablation

Andreas M. Hötker,[1,2] Andreas Meier,[1,2] Yousef Mazaheri,[3] Junting Zheng,[4] Marinela Capanu,[4] Joshua Chaim,[1] Ramon Sosa,[1] Jonathan Coleman,[5] Hedvig Hricak,[1] and Oguz Akin[1]

[1]Department of Radiology, Memorial Sloan-Kettering Cancer Center, 1275 York Ave, New York, NY 10065, USA
[2]Department of Diagnostic and Interventional Radiology, University Hospital Zurich, Rämistrasse 100, 8091 Zurich, Switzerland
[3]Department of Medical Physics, Memorial Sloan-Kettering Cancer Center, 1275 York Avenue, New York, NY 10065, USA
[4]Department of Epidemiology and Biostatistics, Memorial Sloan-Kettering Cancer Center, 1275 York Avenue, New York, NY 10065, USA
[5]Department of Surgery, Urology Service, Memorial Sloan-Kettering Cancer Center, 1275 York Avenue, New York, NY 10065, USA

Abstract

Purpose: The purpose of our study was to retrospectively evaluate and categorize temporal changes in MRI appearances of the prostate in patients who underwent focal therapy with MRI follow-up.
Methods: The Institutional Review Board approved this retrospective study and waived the requirement for informed consent. Thirty-seven patients (median age 61; 48–70 years) with low-to-intermediate-risk, clinically organ-confined prostate cancer underwent focal ablation therapy from 2009 to 2014. Two radiologists reviewed post-treatment MRIs (n = 76) and categorized imaging features blinded to the time interval between the focal therapy and the follow-up MRI. Inter-reader agreement was assessed (kappa) and generalized linear regression was used to examine associations between an imaging feature being present/absent and days between ablation and MRI.
Results: Inter-reader agreement on MRI features ranged from fair to substantial. Edema was found present at earlier times after ablation (median 16–25 days compared to MRIs without edema, median 252–514 days), as was rim enhancement of the ablation zone (18–22.5 days vs. 409–593 days), a hypointense rim around the ablation zone on T2-weighted images (53-57.5 days vs. 279–409 days) and the presence of an appreciable ablation cavity (48.5–60 days vs. 613–798 days, all $p < 0.05$). Enhancement of the ablation zone/scar (553–731 days vs. 61.5–162 days) and the formation of a T2-hypointense scar were found to be present on later MRI scans (514–553 days vs. 29–32 days, one reader).
Conclusions: The MRI appearance of the prostate after focal ablation changes substantially over time. Identification of temporal patterns in the appearance of imaging features should help reduce image interpretation variability and errors when assessing post-therapeutic scans.

Key words: Prostate cancer—Magnetic resonance imaging—Recurrence—Electroporation—Cryosurgery

The majority of men with prostate cancer in the developed world have their disease diagnosed at an early stage, when it is still clinically localized. Prostate MRI has become an important part of the standard of care in identifying target lesions for guided biopsy [1], in staging prostate cancer [2], in active surveillance [3], and in the detection of recurrent cancer [4]. For patients with localized disease, conservative management approaches, such as active surveillance, or minimally invasive approaches, such as focal ablation, may be appealing options [5–7]. As compared to the more traditional treatments for localized disease—radical prostatectomy and radiation therapy—the major advantage of focal therapy is that it offers the possibility of achieving local cancer control with less morbidity and with possibly a higher rate of preservation of erectile, urinary, and rectal

Electronic supplementary material The online version of this article (https://doi.org/10.1007/s00261-018-1715-9) contains supplementary material, which is available to authorized users.

Correspondence to: Andreas M. Hötker; *email:* Andreas.Hoetker@usz.ch

function [6]. Another advantage of focal therapy is that it does not prevent further treatment with radical prostatectomy (RP), radiation therapy (RT), or repeated focal therapy if the disease is not controlled. However, focal therapy for prostate cancer is still considered an emerging approach that requires further technical refinement and clinical development.

One of the factors preventing broad adoption of focal therapy is the lack of established criteria for determining treatment success and conducting post-treatment surveillance. Traditional surveillance based on monitoring of prostate-specific antigen (PSA) levels is not easily applicable after focal therapy due to the variable amounts of prostate tissue remaining in situ [8, 9]. Another possible means of follow-up, prostate biopsy, is prone to sampling error; furthermore, it is not infrequently associated with morbidity and would therefore reduce the main appeal of focal therapy, which is its minimally invasive nature [10, 11]. Imaging, which is elemental in the post-treatment follow-up of many other solid cancers, may offer a solution.

Magnetic resonance imaging (MRI) is already commonly used in both pre- and post-treatment assessments of men with prostate cancer. In men who undergo focal therapy, it may be used not only to direct the therapy but also to assess the extent of prostate ablation and to depict post-treatment complications, if present. A few reports have suggested that MRI, along with PSA monitoring, could be successfully implemented in the follow-up of focal therapy in men with prostate cancer [12–14], and a recent consensus report recommended MRI as an ideal imaging method for follow-up of patients after focal therapy [15]. However, interpretation of MRI after ablation is based on the radiologist's experience [16], and as to our knowledge, there are no established MRI criteria for defining normal post-treatment appearances.

The purpose of our study was to retrospectively evaluate and categorize temporal changes in MRI appearances of the prostate in patients who underwent focal therapy with MRI follow-up. By describing expected chronological changes within the prostate as seen on MRI, we aimed to begin developing standardized terminology that radiologists could use to reduce image interpretation variability and errors.

Materials and methods

Patients and techniques

This retrospective study was compliant with the Health Insurance Portability and Accountability Act. Our institutional review board approved the study and waived the requirement for informed consent. We searched urology databases for the years 2009–2014 and identified patients who met the following inclusion criteria: (1) focal therapy performed at our institution for biopsy-proven, organ-confined, low- to intermediate-risk (Gleason score $\leq 3 + 4$) prostate cancer; (2) availability of at least one post-treatment MRI for review. Four patients were subsequently excluded due to prior androgen-deprivation therapy or prior radiotherapy, and two other patients were excluded from analysis because of several sequential treatments with overlapping ablation zones; in addition, an outside follow-up MRI from one other patient was excluded from analysis due to bad image quality. Patients undergoing laser ablation ($n = 2$) or photodynamic therapy (PDT, $n = 3$) were not included to allow for a more homogeneous study cohort. The final study cohort consisted of 37 men (median age 61; 48–70 years); a total of 76 post-treatment MRIs performed during the follow-up of the patients were included in the analysis. Most patients were followed up with sequential MRI examinations; thus, 10 patients each had a single examination, 16 patients each had two examinations, 10 patients each had 3 examinations, and a single patient had 4 examinations included in the analysis.

Focal ablation techniques used included cryoablation ($n = 12$; 32.4%) and irreversible electroporation (IRE) ($n = 25$; 67.6%).

MRI Technique and Interpretation

All MRIs were performed at field strengths of 1.5T ($n = 8$) or 3T ($n = 68$) using a pelvic phased-array coil. In 38 scans, an endorectal coil was additionally used. Eighty-one of the examinations were performed at our own institution, and 7 were acquired elsewhere. All MRI examinations included at least a T1-weighted sequence in transverse orientation (TR: 4.2 × 5.3 ms, TE: 1.3 × 1.2 ms, flip angle: 12°, matrix: 256 × 128–256 × 160, FoV: 16 × 16 cm, slice thickness: 3 mm) and T2-weighted TSE sequences in axial and coronal orientations (TR: 3000–5900 ms, TE: 104–124 ms, matrix: 320 × 192–320 × 320, FoV: 14 × 14–16 × 16 cm, slice thickness: 3–4 mm), with a small field of view covering the prostate and the periprostatic region. For all but 10 MRI examinations, a T1-weighted dynamic contrast-enhanced sequence covering the pelvis was also acquired (TR: 3–4.2 ms, TE: 0.9–1.4 ms, flip angle: 30°, matrix: 256 × 160, FoV: 24 × 24 cm, slice thickness: 6 mm).

Two readers (AMH and AM), blinded to all clinical information, independently reviewed all scans and evaluated the following qualitative MRI features: (1) presence of a post-treatment cavity, defined as a circumscribed, non- or late-enhancing region; (2) presence of a scar, defined as a T2-weighted marked hypointense, linearly shaped area; (3) visibility of a circumscribed hypointense rim around the ablation zone on T2-weighted images ('dark rim'); (4) presence of fluid in the ablation zone; (5) appreciable edema, defined as diffusely hyperintense area on T2-weighted and diffu-

sion-weighted images with a low b-value; (6) complex fluid (hemorrhagic/proteinaceous fluid), defined as hyperintense areas on T1-weighted images; (7) appreciable rim enhancement around the ablation zone; and (8) appreciable enhancement in the ablation cavity/scar (see Fig. 1A–E for examples of some of these features). These features were defined by two experienced radiologists prior to analysis (AMH and AM), who did not participate as readers in the study. In addition, the prostate volume (using the ellipsoid formula [17]) and the maximal extent of the ablation zone on any plane were measured on the T2-weighted images.

Statistical analysis

For each reader, generalized linear regressions were used to examine associations between days from ablation to MRI and individual quantitative and qualitative MRI features with identity and logit link function, respectively; considering some patients had multiple MRI examinations, the generalized estimating equations (GEE) method was performed with an independent correlation structure and a robust covariance matrix. For continuous size and volume measurement on MRI, the absolute difference and 95% CI were estimated for every 30-day increase in time interval. For presence of edema by reader 1, due to a complete separation where all MRIs with edema had shorter interval from ablation than MRIs without edema, Firth's penalized maximum likelihood estimation was performed. Inter-reader agreement was assessed using kappa statistics and the intraclass correlation coefficient (ICC) for qualitative and quantitative features, respectively. The 95% confidence intervals of kappa and ICC were estimated using the bootstrap method. Kappa (κ) values were interpreted as follows: 0.00–0.20, slight agreement; 0.21–0.40, fair agreement; 0.41–0.60, moderate agreement; 0.61–0.80, substantial agreement; and 0.81–1.00, almost perfect agreement. A test with p value < 0.05 was considered statistically significant. All statistical analyses were performed in software packages SAS 9.4 (SAS Institute Inc., Cary, NC, USA) and R version 3.1 (The R Foundation for Statistical Computing).

Results

Patient characteristics

Of the 37 men included in this study, 26 (70.3%) had prostate cancer with a Gleason score of 3 + 3 and 11 (29.7%) had a Gleason score of 3 + 4. Clinical stage prior to ablation treatment was T1c in all patients and the mean pre-treatment prostate-specific antigen (PSA) value was 6.17 (range 0.83–22.82 ng/mL). For all MRI examinations included, median time between ablation and MRI was 187 (range 8–1859 days).

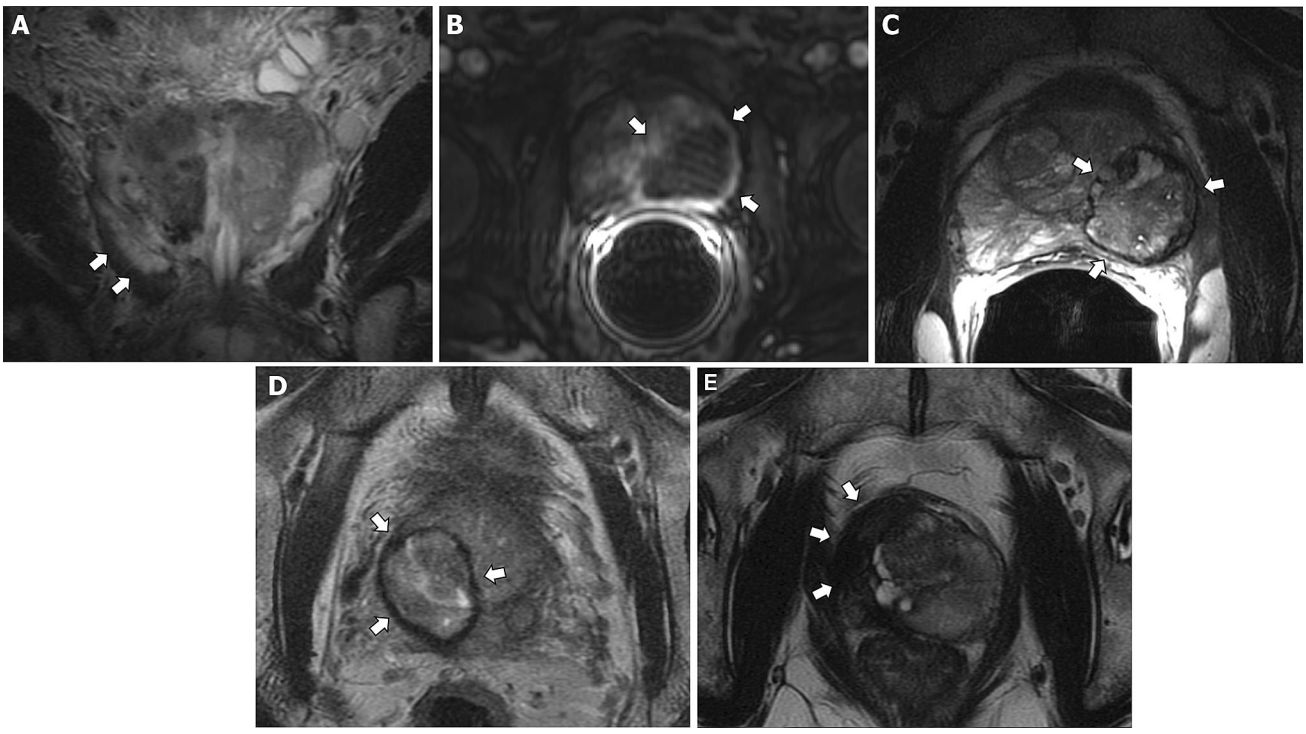

Fig. 1. **A–E** Illustrative examples for the following MRI features: **A** extensive edema after ablation with inclusion of the right levator ani muscle, **B** rim enhancement around the ablation zone, **C**, **D** hypointense rim around the ablation zone on T2-weighted images ('dark rim'), and **E** scarring after ablation at the right side of the prostate.

Inter-reader agreement

Inter-reader agreement on qualitative imaging features ranged from fair (ablation zone enhancement, $\kappa = 0.219$) to substantial (rim enhancement, $\kappa = 0.781$), with most features showing moderate or substantial agreement (see Table 1). Agreement was high (ICC = 0.911) with regard to prostate volume measurement and moderate (ICC = 0.719) with regard to the length of the ablation zone.

Qualitative imaging features

Table 2 lists the associations between the presence or absence of qualitative imaging features and the time between ablation and MRI, and Fig. 2A, B illustrates the distribution of the MRI features along the time axis for both readers. Supplementary Table 1 illustrates the frequencies of features being present/absent in the first three months vs. later after ablation.

For both readers 1 and 2, the presence of edema on MRI was found at the shortest median time interval of 16–25 days (reader 1 and 2) after ablation, compared to MRIs without edema (median 252–514 days, $p < 0.001$), followed by rim enhancement of the ablation zone (18–22.5 vs. 409–593 days), a hypointense rim around the ablation zone on T2-weighted images (53–57.5 vs. 279–409 days), and the presence of an appreciable ablation cavity (48.5–60 vs. 613–798 days, all $p < 0.05$ when comparing to the feature being absent). Features present on later MRI scans were enhancement of the ablation zone (or scar) itself (553–731 vs. 61.5–162 days; $p < 0.03$) and the formation of a T2-hypointense scar (514–553 vs. 29–32 days after ablation); however, the latter feature was only statistically significant for reader 1, with a borderline p value of 0.05 for reader 2.

The presence of complex fluid was only found to be significantly associated with the time after ablation for reader 2 (median of 108 days). The presence of fluid in the ablation zone was not found to be associated with time for either reader.

Quantitative imaging features

Prostate volume was not found to change significantly over time after ablation for either reader, though a trend toward a slight increase over time was visible (see Table 3). For reader 1, a slight decrease of the ablation zone length over time was found to be statistically significant ($p < 0.001$), but this did not hold true for reader 2 ($p = 0.364$).

Table 1. Inter-reader agreement on qualitative and quantitative imaging features

Reader 1	Reader 2		
	No	Yes	
Qualitative features			Kappa (95% CI)
Presence of cavity			
No	18 (24%)	3 (4%)	0.663 (0.454, 0.828)
Yes	8 (11%)	47 (62%)	
Presence of scar			
No	32 (42%)	5 (7%)	0.711 (0.546, 0.862)
Yes	6 (8%)	33 (43%)	
Dark rim			
No	43 (57%)	5 (7%)	0.624 (0.412, 0.782)
Yes	8 (11%)	20 (26%)	
Fluid in ablation zone			
No	39 (51%)	10 (13%)	0.392 (0.166, 0.598)
Yes	11 (14%)	16 (21%)	
Edema			
No	42 (55%)	17 (22%)	0.525 (0.345, 0.689)
Yes	0 (0%)	17 (22%)	
Complex fluid			
No	25 (33%)	18 (24%)	0.411 (0.217, 0.608)
Yes	5 (7%)	28 (37%)	
Rim enhancement			
No	34 (52%)	1 (2%)	0.781 (0.593, 0.92)
Yes	6 (9%)	24 (37%)	
Ablation zone enhancement			
No	43 (66%)	12 (18%)	0.219 (− 0.022, 0.496)
Yes	5 (8%)	5 (8%)	
Quantitative features			ICC (95% CI)
Prostate volume			0.911 (0.865, 0.938)
Length of ablation zone			0.719 (0.599, 0.819)

Table 2. Qualitative MRI features and time between ablation and MRI for both readers, univariate analysis

Qualitative features	Time between ablation and MRI, days		
	Feature absent Median (range), *n*	Feature present Median (range), *n*	*p* value
Reader 1			
Presence of cavity	798 (153, 1859), 21	60 (8, 1092), 55	< 0.001
Presence of scar	29 (8, 713), 37	553 (162, 1859), 39	0.048
Dark rim	409 (8, 1859), 48	57.5 (15, 279), 28	< 0.001
Fluid in ablation zone	186 (8, 1673), 49	188 (14, 1859), 27	0.448
Edema	252 (27, 1859), 59	16 (8, 23), 17	< 0.001
Complex fluid	398 (10, 1859), 43	55 (8, 1673), 33	0.120
Rim enhancement	593 (153, 1859), 46	22.5 (8, 420), 41	0.036
Ablation zone enhancement	162 (8, 1859), 66	731 (174, 1557), 21	0.003
Reader 2			
Presence of cavity	613 (153, 1673), 26	48.5 (8, 1859), 50	0.006
Presence of scar	32 (8, 1092), 38	514 (174, 1859), 38	0.050
Dark rim	279 (8, 1859), 51	53 (16, 593), 25	0.003
Fluid in ablation zone	174.5 (8, 1673), 50	205.5 (14, 1859), 26	0.744
Edema	514 (36, 1859), 42	25 (8, 398), 34	< 0.001
Complex fluid	461 (13, 1859), 30	108 (8, 1673), 46	0.024
Rim enhancement	409 (36, 1859), 51	18 (8, 299), 36	0.002
Ablation zone enhancement	61.5 (8, 1673), 59	553 (36, 1859), 28	0.026

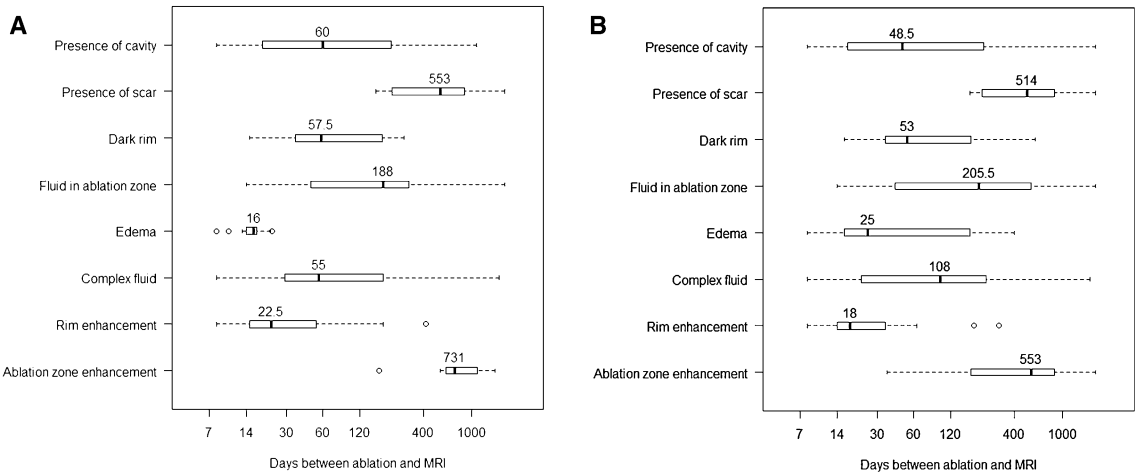

Fig. 2. **A**–**B** Graphical illustrations of the temporal distribution of MRI features for reader 1 (**A**) and reader 2 (**B**).

Table 3. Quantitative MRI features and time between ablation and MRI (R1 = reader 1, R2 = reader 2; prostate volume in ml, length of ablation zone in cm)

Quantitative features	Mean ± SD, median (range)	Size difference[a] (95% CI) per every 30-day increase in time between ablation and MRI	*p* value
Prostate volume (R1)	38.5 ± 17.1, 36.5 (10, 82)	0.11 (− 0.10, 0.32)	0.323
Length of ablation zone (R1)	3 ± 1.1, 2.9 (0.9, 6.7)	− 0.021 (− 0.033, − 0.009)	< 0.001
Prostate volume (R2)	42.3 ± 17.8, 39.5 (14, 99)	0.08 (− 0.12, 0.28)	0.441
Length of ablation zone (R2)	3.1 ± 0.8, 3.2 (1.6, 5.5)	− 0.004 (− 0.013, 0.005)	0.364

[a]Size difference is the estimated mean difference of sizes measured on MRI (size of longer time interval − size of shorter time interval)

Discussion

Focal ablation of prostate cancer has emerged as a new, more conservative treatment option for a subset of patients with less aggressive and localized disease [7, 18]. Although long-term oncological follow-up data are still sparse, this new treatment approach seems to offer reduced morbidity compared to radical prostatectomy, as the image-guided nature of focal therapy allows for delivering treatment to the tumor region while sparing surrounding critical structures such as the neurovascular bundles (NVB), the urinary sphincter, the bladder neck, and the rectum. Most importantly, initial ablation does not preclude the later use of more radical surgery in patients with, e.g., local recurrence or residual disease. However, this less invasive approach requires continued follow-up to avoid under-treatment and to identify disease in an early stage that still allows for additional treatment (i.e., subsequent ablation, surgical resection). The standard workup for recurrence or the proliferation of cancer foci left untreated based on PSA measurements has been found to be inconclusive, as patients undergoing focal ablation retain a significant part of their prostatic tissue [8, 9]. Repeated biopsy without suspicion of recurrence or tumor growth, on the other hand, would negate the concept of a less invasive approach and may be prone to sampling error [10, 11].

Serial MRI may offer a means of achieving practical and effective post-treatment surveillance, as it can be used to assess for recurrent/residual tumor non-invasively and, when necessary, guide a targeted biopsy of a suspicious area. Consequently, it has recently been endorsed by an international consensus project [15]. However, assessment of prostate MRI in general, and especially after ablation, is strongly dependent on the individual radiologist's experience [16, 19], and moreover, because follow-up examinations may not be performed at the same center where the patient was treated, access to prior examinations may be limited. Although the visible changes after focal ablation of the prostate vary strongly, we found them to demonstrate temporal patterns that might help the radiologist by establishing what imaging features to expect after an ablation. For example, we found that the presence of edema was found present at earlier times after ablation (median time intervals of 16 and 25 days after ablation, for the two readers), often together with a rim of enhancement around the ablation zone (likely due to reactive changes of the surrounding tissue resulting from the induced necrosis) [20]. This visibility of a hypointense rim around the ablation zone on T2-weighted images was also found at earlier times after ablation (median 53–57.5 days), probably caused by (chronic) hemorrhage. The latter finding aligns well with the study results reported by van den Bos et al. [21], who correlated MRI findings at a single time point 4 weeks after IRE with histopathological workup after prostatectomy, and who reported a "central white necrotic zone surrounded by an outer, dark red hemorrhagic zone" as a typical appearance of the ablation zone on gross pathology. In our study, the presence of the 'dark rim sign' seemed to co-occur temporally with the formation of a clearly demarked ablation cavity and possibly complex (hemorrhagic/proteinaceous) fluid, whose presence as hyperintense areas on T1-weighted images might possibly indicate hemorrhage into the cavity at a later time after ablation (given that the time interval after ablation extended to 108 days for reader 2). In the later stages of transformation after ablation, the development of scarring, defined as hypointense, linearly shaped areas on T2-weighted images, can be seen (median 514–553 days), along with a discrete enhancement of the ablation zone after application of a contrast agent (553–731 days).

The presence of fluid in the ablation area was not found to be statistically significantly associated with the time after ablation; the reason for this lie in the fact that this imaging feature could be visible at different time points for different reasons—e.g., after formation of an ablation cavity or, for example, in case of involvement of the urethra in the ablation zone.

Although prostate volume did not change significantly over the course of the follow-up, a slight trend toward an increase in volume over time was visible for both readers; this increase might be due to the expected recovery of the prostatic tissue. The lack of statistical significance may reflect the fact that the ablation zone—and therefore the likelihood and degree of change in prostate volume—differed between individual patients. For one reader, the length of the ablation zone showed a statistically significant slight decrease over time, which probably relates to scarring.

Our study had a number of limitations. Due to the uneven distribution of ablation techniques used, we were not able to compare MRI findings between patients treated with different methods. Given the different mechanisms of action of IRE and cryoablation, future studies investigating the different techniques separately are certainly warranted, as the differences among the biological changes induced by the different techniques may also be reflected in the imaging features visible on MRI. In addition, this study represents a retrospective assessment of patients undergoing focal therapy for prostate cancer as a minimally invasive form of treatment, so correlation of MRI and histopathological features was not possible. Finally, we included not only MRI examinations obtained at our institution with a standardized MR protocol, but also a few examinations from outside institutions, if performed as dedicated prostate MRI examinations. While we could not account for differences between scans obtained at our institution and those obtained elsewhere (e.g., due to differences in MRI vendors), we believe the influences of such differ-

ences were likely minimal since our study relied on the qualitative assessment of imaging features on post-treatment scans.

In conclusion, this study identified temporal patterns in the appearance of MRI features during the follow-up of patients who have undergone focal ablation for prostate cancer. Radiologists' awareness of these temporal patterns could reduce image interpretation variability and errors, thus increasing the value of MRI in post-ablation follow-up.

Acknowledgements The authors thank Ada Muellner, MS for editing the manuscript.

Compliance with ethical standards

Funding This research was funded in part through the NIH/NCI Cancer Center Support Grant P30 CA008748.

Conflicts of interest All authors declare no conflict of interest.

Research involving human participants All procedures performed in studies involving human participants were in accordance with the ethical standards of the institutional and/or national research committee and with the 1964 Helsinki declaration and its later amendments or comparable ethical standards.

Informed consent The requirement for informed consent was waived by the local IRB for this retrospective study.

References

1. Ahmed HU, El-Shater Bosaily A, Brown LC, et al. (2017) Diagnostic accuracy of multi-parametric MRI and TRUS biopsy in prostate cancer (PROMIS): a paired validating confirmatory study. Lancet 389(10071):815–822. https://doi.org/10.1016/S0140-6736(16)32401-1
2. Somford DM, Hamoen EH, Fütterer JJ, et al. (2013) The predictive value of endorectal 3 Tesla multiparametric magnetic resonance imaging for extraprostatic extension in patients with low, intermediate and high risk prostate cancer. J Urol 190(5):1728–1734. https://doi.org/10.1016/j.juro.2013.05.021
3. Klotz L, Vesprini D, Sethukavalan P, et al. (2015) Long-term follow-up of a large active surveillance cohort of patients with prostate cancer. J Clin Oncol 33(3):272–277. https://doi.org/10.1200/JCO.2014.55.1192
4. Oppenheimer DC, Weinberg EP, Hollenberg GM, et al. (2016) Multiparametric magnetic resonance imaging of recurrent prostate cancer. J Clin Imaging Sci 6:18. https://doi.org/10.4103/2156-7514.181494
5. Ahmed HU, Hindley RG, Dickinson L, et al. (2012) Focal therapy for localised unifocal and multifocal prostate cancer: a prospective development study. Lancet Oncol 13(6):622–632. https://doi.org/10.1016/S1470-2045(12)70121-3
6. Valerio M, Cerantola Y, Eggener SE, et al. (2016) New and established technology in focal ablation of the prostate: a systematic review. Eur Urol . https://doi.org/10.1016/j.eururo.2016.08.044
7. Ahmed HU, Dickinson L, Charman S, et al. (2015) Focal ablation targeted to the index lesion in multifocal localised prostate cancer: a prospective development study. Eur Urol 68(6):927–936. https://doi.org/10.1016/j.eururo.2015.01.030
8. Barret E, Harvey-Bryan K-A, Sanchez-Salas R, et al. (2014) How to diagnose and treat focal therapy failure and recurrence? Curr Opin Urol 24(3):241–246. https://doi.org/10.1097/MOU.0000000000000052
9. Bozzini G, Colin P, Nevoux P, et al. (2013) Focal therapy of prostate cancer: energies and procedures. Urol Oncol 31(2):155–167. https://doi.org/10.1016/j.urolonc.2012.05.011
10. Welch HG, Fisher ES, Gottlieb DJ, et al. (2007) Detection of prostate cancer via biopsy in the medicare-SEER population during the PSA era. J Natl Cancer Inst 99(18):1395–1400. https://doi.org/10.1093/jnci/djm119
11. Mian BM, Lehr DJ, Moore CK, et al. (2006) Role of prostate biopsy schemes in accurate prediction of Gleason scores. Urology 67(2):379–383. https://doi.org/10.1016/j.urology.2005.08.018
12. Kirkham APS, Emberton M, Hoh IM, et al. (2008) MR imaging of prostate after treatment with high-intensity focused ultrasound. Radiology 246(3):833–844. https://doi.org/10.1148/radiol.2463062080
13. Rosenkrantz AB, Scionti SM, Mendrinos S, et al. (2011) Role of MRI in minimally invasive focal ablative therapy for prostate cancer. AJR Am J Roentgenol 197(1):W90–W96. https://doi.org/10.2214/AJR.10.5946
14. de Visschere PJ, de Meerleer GO, Futterer JJ, et al. (2010) Role of MRI in follow-up after focal therapy for prostate carcinoma. AJR Am J Roentgenol 194(6):1427–1433. https://doi.org/10.2214/AJR.10.4263
15. Muller BG, van den Bos W, Brausi M, et al. (2015) Follow-up modalities in focal therapy for prostate cancer: results from a Delphi consensus project. World J Urol 33(10):1503–1509. https://doi.org/10.1007/s00345-014-1475-2
16. Akin O, Riedl CC, Ishill NM, et al. (2010) Interactive dedicated training curriculum improves accuracy in the interpretation of MR imaging of prostate cancer. Eur Radiol 20(4):995–1002. https://doi.org/10.1007/s00330-009-1625-x
17. Weinreb JC, Barentsz JO, Choyke PL, et al. (2016) PI-RADS prostate imaging—reporting and data system: 2015, version 2. Eur Urol 69(1):16–40. https://doi.org/10.1016/j.eururo.2015.08.052
18. Eggener SE, Yousuf A, Watson S, et al. (2016) Phase II evaluation of magnetic resonance imaging guided focal laser ablation of prostate cancer. J Urol . https://doi.org/10.1016/j.juro.2016.07.074
19. Wibmer A, Vargas HA, Donahue TF, et al. (2015) Diagnosis of extracapsular extension of prostate cancer on prostate MRI: impact of second-opinion readings by subspecialized genitourinary oncologic radiologists. AJR Am J Roentgenol 205(1):W73–W78. https://doi.org/10.2214/AJR.14.13600
20. Bomers JGR, Cornel EB, Futterer JJ, et al. (2016) MRI-guided focal laser ablation for prostate cancer followed by radical prostatectomy: correlation of treatment effects with imaging. World J Urol . https://doi.org/10.1007/s00345-016-1924-1
21. van den Bos W, de Bruin DM, van Randen A, et al. (2016) MRI and contrast-enhanced ultrasound imaging for evaluation of focal irreversible electroporation treatment: results from a phase I-II study in patients undergoing IRE followed by radical prostatectomy. Eur Radiol 26(7):2252–2260. https://doi.org/10.1007/s00330-015-4042-3